SIXTH EUROPEAN ROTORCRAFT AND POWERED LIFT AIRCRAFT FORUM

PAPER NO. 41

FLIGHT INVESTIGATIONS OF A HELICOPTER LOW AIRSPEED ESTIMATION SYSTEM BASED ON MEASUREMENT OF CONTROL PARAMETERS

A.J. Faulkner
F. Buchner

Messerschmitt-Bölkow-Blohm GmbH
Munich, Germany

September 16 - 19, 1980
Bristol, England

THE UNIVERSITY, BRISTOL, BS8 1HR, ENGLAND

FLIGHT INVESTIGATIONS OF A HELICOPTER LOW AIRSPEED ESTIMATION SYSTEM BASED ON MEASUREMENT OF CONTROL PARAMETERS

A.J. Faulkner F. Buchner

Messerschmitt-Bölkow-Blohm GmbH
Munich, Germany

Abstract

Helicopter handling qualities are subject to substantial changes in the form of control sensitivities, control couplings, trim positions and power settings in the hover and the low flight speed region. In addition, the piloting task is very often compounded by the mission - for example, winching, landing, confined approach - so that the pilot work-load in and around the hover may be considerable. The pilot could well be aided if he were provided with an indication of airspeed, since the handling characteristics are primarily dependent on the rotor inplane component of airspeed. Unfortunately, the conventional pitot-static airspeed sensor operates inadequately at low speeds.

This paper describes an indirect method of airspeed estimation, particularly suitable for the modern hingeless rotor helicopter, based on the measurement of control and other parameters, most of which are readily available in a flight control system. A brief outline of the theory is given and experimental results obtained with a BO 105 helicopter are presented for trimmed and transient flight states in and out of ground effect. Particular attention is given to the rotor down-wash model. The computer hardware, a 16 bit microprocessor, is described.

Notation

a		Blade lift-curve slope
C_T		$= T / \frac{1}{2}\rho \cdot \pi \cdot R^2 (\Omega \cdot R)^2$, thrust coefficient
c	[m]	Blade chord
E_x, E_y		Glauert downwash factors
f_x, f_y, f_z		Functions used in the calculation of airspeed
I_β		Blade second moment of mass
n		Number of blades
n_β		$= \gamma/8$, blade mass number
p	[rad/s]	Roll rate
$\bar{p}$		$= p/\Omega$, non-dimensional roll rate
q	[rad/s]	Pitch rate
$\bar{q}$		$= q/\Omega$, non-dimensional pitch rate
R	[m]	Rotor radius

S_β		$(\bar{\omega}_\beta^2-1)/n_\beta$, blade stiffness number
T	[N]	Rotor thrust
V	[m/s]	Velocity
$\bar{V}$		$= V/\Omega \cdot R$, non-dimensional velocity
V_{Io}	[m/s]	Rotor induced velocity
V_x	[m/s]	Velocity, longitudinal axis
V_y	[m/s]	Velocity, lateral axis
$\beta(\psi)$	[rad]	$\beta_o+\beta_{1s}\cdot\sin\psi+\beta_{1c}\cdot\cos\psi$, blade flapping angle
β_I	[rad]	Rotor in-built coning angle
γ		$= \rho \cdot c \cdot a \cdot R^4/I_\beta$ = Lock's number
$\theta(\psi)$	[rad]	$= \theta_t+\theta_{1s}\cdot\sin\psi+\theta_{1c}\cdot\cos\psi$, blade pitch angle
θ_t	[rad]	In-built blade twist
ρ	[kg/m^3]	Air density
σ		$= n \cdot c \cdot R/\pi \cdot R^2$
ψ	[rad]	Blade azimuth position, zero at rear of disc
Ω	[rad/s]	Rotor angular velocity
ω_β	[rad/s]	Blade natural flapping frequency
$\bar{\omega}_\beta$		$= \omega_\beta/\Omega$, non-dimensional flapping frequency
-		Non-dimensional quantity.

1. Introduction

The control characteristics of the helicopter are significantly influenced by the aerodynamic velocity in the plane of the rotor disc. This is particularly evident in hover, low speed and transition where only small changes in airspeed are rapidly followed by substantial changes in control sensitivities, couplings and trim positions. Considering that one of the main reasons for operating a helicopter is its unique abilities in hover and low speed flight, it is unfortunate that in the very speed range where the pilot is likely to be called upon to perform a task - such as stores positioning, winching, rescue - the piloting operation is one of the most difficult. With training, pilots are able to master the necessary skills, but with increasing emphasis being placed on IFR flight and military missions where ideal flight conditions cannot be guaranteed, an inappropriate use of the controls in emergency under stress conditions could prove fatal.

As an aid to the piloting task, an indication of airspeed would appear helpful but the conventional pitot-static sensor is ineffective at airspeeds below about 40 kts. and does not function at all during rearward flight. A Doppler navigation system is unable to be of use since only speed relative to the ground is measured and prevailing wind conditions can easily exceed the airspeed range in question.

Recognising the importance of this lack of instrumentation, various avionic equipment manufacturers, including Marconi Elliot Ltd., J-TEC Associates Inc. and Pacer Systems Inc., have proposed and developed a number of instruments, most of which are based on a modified pitot-static principle.

In a previous paper [1] presented at the Fifth European Rotorcraft and Powered Lift Aircraft Forum, the possibility of estimating the airspeed from the measurement of the control positions was discussed and the method supported with results from simulation studies. This present paper reports on the results of flight tests after a brief review of the method and the mathematical equations involved.

2. Theoretical Analysis

The speed range of interest is more precisely defined by Figure 1. For reasons of safety, performance limitations and control authorities, rearward, lateral and vertical velocities are limited to a maximum of about 20 m/s and 10 m/s respectively. In most instances, the appropriate pilots' flight handbook will impose further limitations on the permissible airspeed so that a maximum of 10 m/s to the rear and about 15 m/s sideways are probably more realistic limits.

Cyclic control requirements for trim are typified by Figure 2. Of particular interest is that the cyclic trim position for low forward speeds contains a significant lateral component, in some cases greater than the expected corresponding longitudinal displacement. To initiate a manoeuvre however, pilots' control inputs are essentially in the expected sense, but, as the forward speed increases, the trim requirements necessitate a substantial lateral input. The characteristics described above are similarly reflected in the other three flight directions, slight differences occuring as a result of dissymmetry in fuselage aerodynamics and interference effects.

Since airspeed substantially affects control trim position, it can be concluded that measurement of control position can be used to estimate airspeed. Unfortunately, a simple calibration of airspeed with respect to cyclic position is not sufficient, since other factors such as flight mass and mass-centre position, which are likely to change during flight, also have an effect on trim position. However, these effects can be essentially compensated by measuring the rotor response as well as control inputs. It is thus necessary to construct a suitable mathematical model of the rotor system and invert the equations to solve for airspeed.

Current mathematical models of the helicopter rotor, as used in rotor performance, stability and blade dynamic calculations, have been developed over a number of years and, in an attempt to accurately predict the limits of the rotor, they have inevitably expanded dramatically in complexity (to include non-linear aerodynamics, blade couplings and elastic effects) in proportion to the computing capacity available. The level of complexity, as required for modern rotorcraft design, renders them quite useless for the purpose of the inverse problem of estimating airspeed. Therefore a much simplified model is required, while remembering that non-linear effects need not be considered since the rotor will not be operating at any limiting conditions in the speed range of interest. A detailed

analysis, which essentially involves a simplified analytic solution of the rotor flapping and thrust equations, is given in [1]. Inverting the equations and making appropriate approximations for second order quantities leads to the following expressions for the longitudinal and lateral aerodynamic velocity components in non-dimensional form,

$$\bar{V}_x = \bar{f}_x - \bar{f}_z \cdot \bar{f}_y$$

$$\bar{V}_x = \bar{f}_z \cdot \bar{f}_x + \bar{f}_y$$

where

$$\bar{f}_x = \frac{S_\beta \cdot \beta_{1s} - \beta_{1c} - \theta_{1s} - \bar{p} + \frac{2}{n_\beta} \cdot \bar{q} + E_y \cdot \bar{V}_{Io}}{\theta_t + \frac{4}{3}\theta_o + \frac{4C_T}{a \cdot \sigma}}$$

$$\bar{f}_y = \frac{\beta_{1s} + S_\beta \cdot \beta_{1c} - \theta_{1c} - \frac{2}{n_\beta} \cdot \bar{p} - \bar{q} + E_x \cdot \bar{V}_{Io}}{\theta_t + \frac{4}{3}\theta_o + \frac{4C_T}{a \cdot \sigma}}$$

$$\bar{f}_z = \frac{\frac{4}{3}(\beta_I + \beta_o)}{\theta_t + \frac{4}{3}\theta_o + \frac{4C_T}{a \cdot \sigma}}$$

Measurement is required for the collective (θ_o) and cyclic (θ_{1s}, θ_{1c}) control angles, rotor harmonic flapping coefficients (β_{1s}, β_{1c}) and angular rates (p, q). The stiffness number (S_β), blade mass number (n_β), lift-curve slope (a), rotor solidity (σ) and blade twist (θ_t), can be defined for a particular helicopter. Thrust coefficient, though strictly a function of helicopter mass and altitude can be evaluated for average values. The downwash terms ($E_x \cdot \bar{V}_{Io}$, $E_y \cdot \bar{V}_{Io}$) are significant and discussed in some depth in section 3·3.

Turning to the problem of implementing the method, measurement of control positions and angular rates presents no great problems and in fact these are often available as part of an automatic flight control system. A number of possibilities exist for measuring rotor blade flapping. In the case of a fully articulated rotor, it is conceivable to measure the blade flap angle directly at the flapping hinge with perhaps an inductive type sensor. With a hingeless rotor, by definition no physical hinge exists (though an equivalent hinge off-set is often quoted) and some other means must be sought. Without great inaccuracy it is possible to relate the blade bending moment in the flapping direction to the blade angle, or alternatively the difference in bending moment between two opposing blades can be measured, thus eliminating the non-harmonic component. This latter method was used during the experimental investigation, since in order to monitor hub loads,

a moment sensor, fitted inside the rotor mast, forms part of the standard instrumentation fit on the MBB BO 105 helicopter. Rotating with the rotor, the sensor supplies an essentially once-per-rev. harmonic moment superimposed with 4Ω and higher harmonics as shown in Figure 3. By appropriate filtering of this signal to eliminate higher harmonics, and evaluating a rotor "stiffness" constant, it is possible to evaluate the required first harmonic flapping components β_{1s}, β_{1c}. Figure 4 shows the location of the mast moment sensor which was so arranged, for the experimental investigations, that when in the righthand side position, a marker pulse was triggered to identify the azimuth angle.

A schematic of the system principle is given as a summary in Figure 5.

3. Experimental Investigations

3.1 Flight Programme

The experimental investigations were performed with a PAH-1, an anti-tank derivative of the BO 105 helicopter (Figure 6). The PAH-1 was chosen for the tests since it is equiped with a Singer Kearfott LDNS (Lightweight Doppler Nav. System) ASN 128 and a precision automatic heading stabilization system. The Doppler was required as a reference signal with which to compare the calculated airspeed, and the heading stabilization system eased the pilot's task of flying in a continuous straight line (particularly difficult in sideways and rearward flight). Furthermore, the V4 (helicopter serial number) had been used for type testing and was already partially instrumented.

It was necessary to perform the tests with zero wind conditions in order that the Doppler measurements could be interpreted directly as true airspeed. Completely calm conditions proved difficult to find but we were able to achieve wind conditions below a steady 2 kts. The flights took place along a marked concrete runway which assisted the pilot in maintaining a straight flight path. The pilot was briefed to accelerate from hover to the reference speed and maintain a constant value, with the help of the Doppler system, for approximately 15-20 s. The measurements were repeated at 5 m/s intervals in the longitudinal and lateral directions until the permissible speed limits were reached. Flight was performed both in and out of ground effect and at two typical mass-centre positions (a nominal 11 cm and a 0 cm infront of the rotor axis). All measured values were recorded on an on-board flight recorder.

3.2 Cyclic Trim Requirements

Typical measurements for the cyclic control angles and mast moment are shown in Figure 7, which corresponds to hover with the forward mass-centre position. Owing to the mass-centre off-set, mast moment for trim is not zero and the pilot is required to maintain a rearward cyclic stick input.

Analysis of the measurement recordings produced the predicted form for the cyclic trim curves (Figure 8). Although not directly comparable, owing to differences in aircraft mass and mass-centre, the measurements agree favourably with the theoretical curve (Figure 2). The curve is displaced rearward from the origin owing to the forward mass-centre position.

A movement of the mass-centre (Figure 9) produces an almost identical curve but centred about a different control value.

From both figures it is evident that aerodynamic dissymmetry of the fuselage generates different control requirements for forward and rearward flight. The PAH-1 horizontal tailplane is situated towards the end of the tailboom so that in hover it receives only the edge of the rotor downwash. At low forward speed the tailplane is completely in the rear of the rotor downwash and at higher speed downwash has less effect on the tailplane. There is a tendency therefore, for the cyclic trim points between about 10 and 30 m/s to accumalate in one region in forward flight.

The cyclic trim curve in ground effect (Figure 10) has distinct differences. Between hover and 5 m/s the magnitude of the cyclic input is smaller in comparison to that out of ground effect. Furthermore, the lateral cyclic trim input is less in this region. The same phenomenon was reported by Sheridan and Wiesner [2], who performed wind tunnel measurements on a YUH-61A model in ground effect, and is attributed to the ground vortex which forms infront of the rotor. The vortex, the position of which is a function of forward speed, changes the angle of attack when under the leading edge of the rotor with consequent change in the blade lift force.

3.3 Estimation of Airspeed

The equations for calculating the airspeed (as described in Section 2) were programed on a special purpose digital micro-computer along with the necessary control and interrupt routines. Advantage was taken of the flexibility of the computer to build in a range of values, which could be selected at will, for the fixed coefficients.

The system compensates for the effects of mass-centre variation (comparison between Figures 8 und 9 shows these as not negligible) by measuring the rotor response; in this case mast moment is measured and translated into rotor flap angle. The importance of including this term can be seen from Figure 11. The calculated forward speed compared with the Doppler signal as reference is more negative, as would be expected when rotor flapping is not included. The effect is more pronounced in rearward flight since the trim requirements are for a positive pitching moment at the rotor hub. In forward flight the rotor hub moment is smaller (because of the fuselage aerodynamic characteristics) and the two curves tend to a common value.

The calculated lateral component of airspeed (Figure 12), for the same longitudinal speed range discussed above, is primarily dependent on the downwash model. In hover it can reasonably be assumed that the downwash field is uniform across the complete rotor disc. In translational flight, this assumption is no longer valid and, if used, leads to completely erroneous calculations. In practice, the downwash is reduced at the leading edge and increased at the trailing edge of the rotor disc in forward flight. For normal flight mechanic calculations it is usual to assume a trapezoidal velocity distribution across the rotor disc (Figure 13) as originally proposed by Glauert. The problem is to evaluate the Glauert downwash factor (E), defining the trapezoidal form, a problem

yet to be completely resolved. Harris [3] performed a set of wind tunnel tests and compared measured cyclic trim angles with theoretical predictions from downwash models proposed by Coleman, Castles and De Leeuw and others. None of the models satisfactorily agreed with the wind tunnel measurements. White [4] extended the work with a relatively simple equation with some better agreement.

With this bachground of uncertainty, and recognising the importance of this parameter in the trim equations, it was decided to program a variable function into the computer and experiment with the equations. A simple,

$$E_x = \frac{1}{2} \cdot \frac{V_x}{V_{Io}}$$

was found to be insufficient,

$$E_x = \frac{V_x}{V_{Io}}$$

was found to be better, though this led to a greater overcompensation with increase in speed (Figure 12). It may be concluded that somewhere between these two forms an acceptable curve form can be found, perhaps with a steeper initial gradient, gradually reducing with speed. Interestingly enough this conclusion compares favourably with the proposal of White (Figure 14) whereas another common model given in Payne [5]

$$E_x = \frac{4}{3} \frac{V_x}{V_{Io}} \cdot \frac{1}{1,2 + \frac{V_x}{V_{Io}}}$$

gives a consistently too low value for Ex. These results tend to be substantiated by a completely separate study on the MBB/Kawasaki BK 117, where downwash factors in value similar to White's predictions were required in the flight mechanics programs in order to compare with flight test measurements.

In sideways flight, the calculated speed corresponds with reasonable accuracy (Figures 15 and 16) to the Doppler speeds. There is a tendency for increased errors at about 15 m/s, which are most likely due to inaccuracies in the downwash model described above.

The results in ground effect tended to show greater discrepancies, but it must be recognised that the pilot was naturally more cautious while flying at less than 2 m above the ground and was not always able to maintain the flight speed. Typical results are given in Figures 17 and 18 for the longitudinal speed case.

Good dynamic response was obtained as demonstrated in Figure 19. The transition from rearward flight to forward flight shows close agreement with the Doppler signals. As a further example Figure 20 shows the results during a turn and re-positioning manoeuvre on the helicopter reaching the end of the runway.

In summary, the experimental investigation has demonstrated the feasibility of the method and has shown promising results. It can reasonably be expected that with more work on parameter adjustment and, in particular, on the downwash model, together with improvements in the instrumentation, better accuracy can be obtained.

4. Computer Hardware

The experimental programme required a flexible computer system so that changes in the coefficients could be easily incorporated. For this reason, the equations were programed on a digital computer with the higher frequency filtering operations performed with conventional analogue circuitry. The opportunity was used to implement MODUS (Modulares Digitales Universal-System), a recent MBB developed micro-computer system. MODUS is one of the few currently available 16-bit word micro-computer systems and consists of a complete range of specialised hardware models plus software operating system. MODUS was developed with the specific intention of providing a complete computer system, as opposed to discrete pieces of circuity which must be integrated into a functional unit. Particular attention was paid to provide an architecture which can take into account developments in semiconductor technology that are likely to occur in the foreseeable future. The system is independent of a single manufacturers components, two alternative processor units being currently available based on the Texas Instruments TI SBP 9900 and the Micro Devices AMD 2900 microprocessors. The assembler compiler is available for several host computers and differences in format between manufacturers for the assembler instructions have been eliminated by a common MODUS assembler language. Modification of the original assembler program is therefore not required if the processor is updated to a newer unit, thus saving on the cost of software development. The system is flexible enough to permit multiprocessor operation as well as module redundancy.

For the purposes of our experiments a MODUS micro-computer was configured in very conventional fashion with a 32 channel analogue to digital converter (ADC) for the input signals (cyclic control positions etc.), a SBP 9900 processor with 1 k random access memory (RAM), 8 k x 16-bit erasable programable read only memory (EPROM) for the program instructions, 4 channel digital analogue converter (DAC) for the output signals, and associated bus controller and power supplies. A schematic of the system structure is given in Figure 21. The MODUS computer provided adequate capacity with about 1,7 k words of memory required for the program instructions with an additional 1,5 k for the monitor. The complete computer was assembled in a standard commercial 19" chassis with the front panel being used for mounting connectors and potentiometers for varying the coefficient values (Figure 22).

5. Conclusions

The experimental investigations have demonstrated the feasibility of estimating the helicopter airspeed from measurement of control inputs and helicopter response. It is to be expected that with further parameter "tuning" and with perhaps improvements in instrumentation better accuracy can be achieved.

As a by-product of the investigations, useful information has been gathered to support doubts about some of the common downwash models and it is clear that further wind tunnel experimental work is required in this area before rotor downwash characteristics can confidently be predicted.

6. References

1. A.J. Faulkner, S. Attlfellner — A Method of Helicopter Low Airspeed Estimation based on Measurement of Control Parameters. Fifth European Rotorcraft and Powered Lift Aircraft Forum (1979) Paper 31

2. P.F. Sheridan, W. Wiesner — Aerodynamics of Helicopter Flight Near the Ground. 33rd. Annual National Forum of the American Helicopter Society (1977) Preprint 77.33.04

3. F.D. Harris — Articulated Rotor Blade Flapping Motion at Low Advance Ratio. J. of American Helicopter Society (1972) Vol. 17 No. 1 41-48

4. F. White, B.B. Blake — Improved Method of Predicting Helicopter Control Response and Gust Sensitivity 35th. Annual National Forum of the American Helicopter Society (1979) Preprint 79.25

5. P.R. Payne — Helicopter Dynamics and Aerodynamics Sir Isaac Pitman & Sons Ltd. (1959).

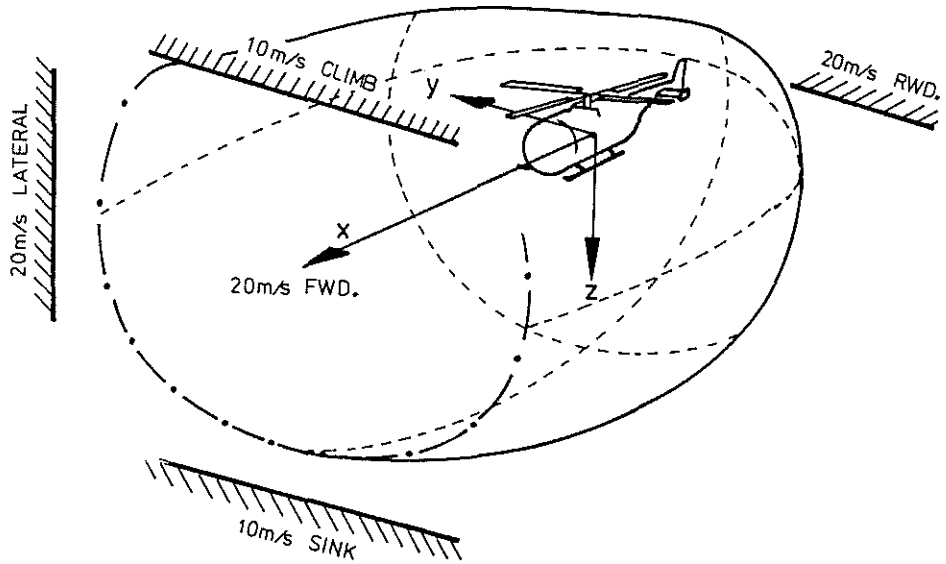

Figure 1 Low Speed Flight (Typical Velocity Limits)

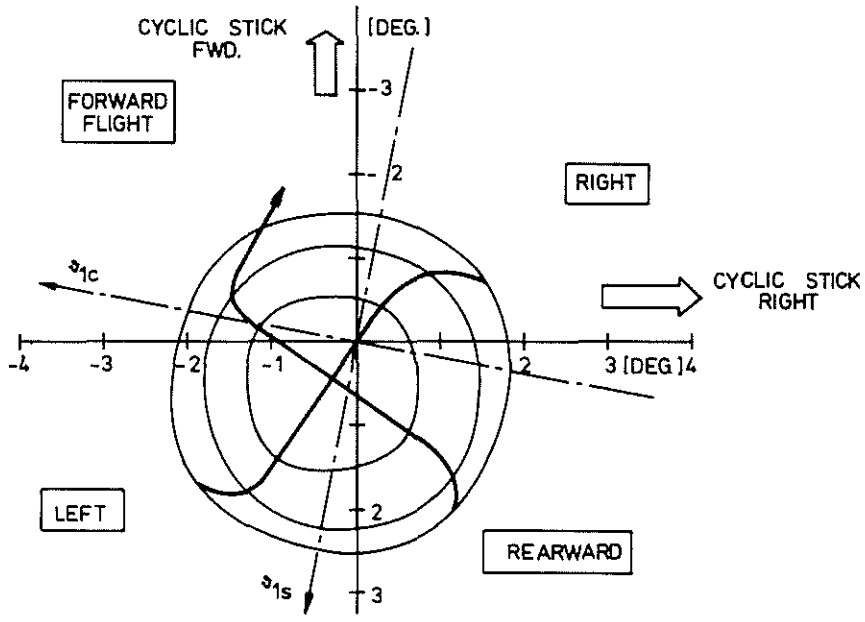

Figure 2 Typical Cyclic Control Requirements for Trim

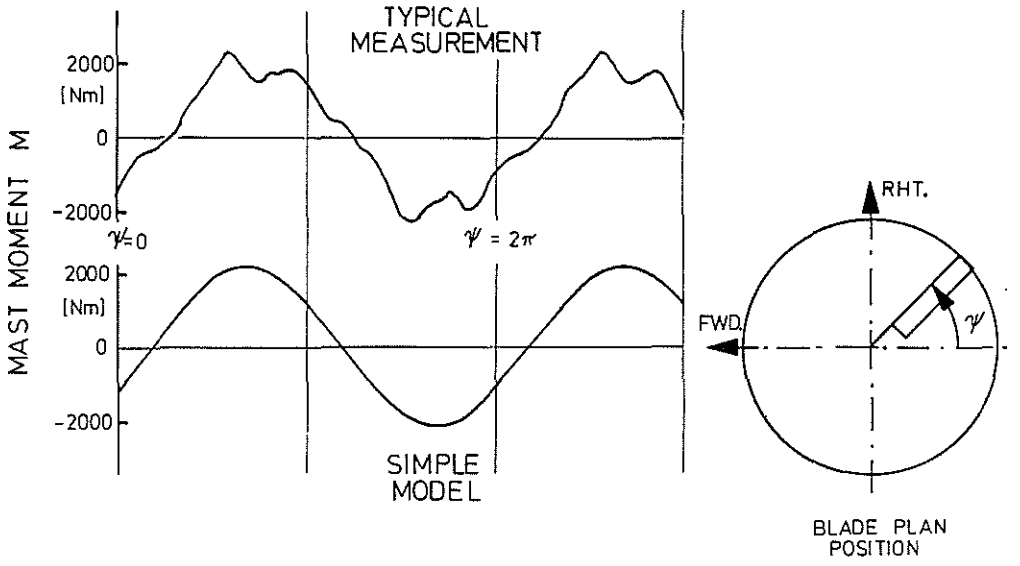

Figure 3 Rotor Mast Moment vs. Azimuth Angle

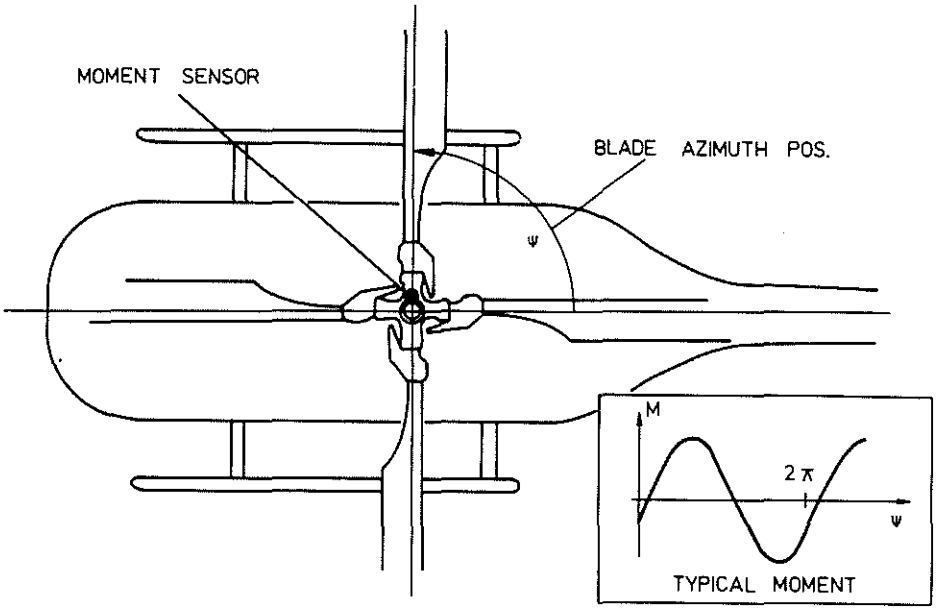

Figure 4 Schematic Showing Measurement of Rotor Mast Moment

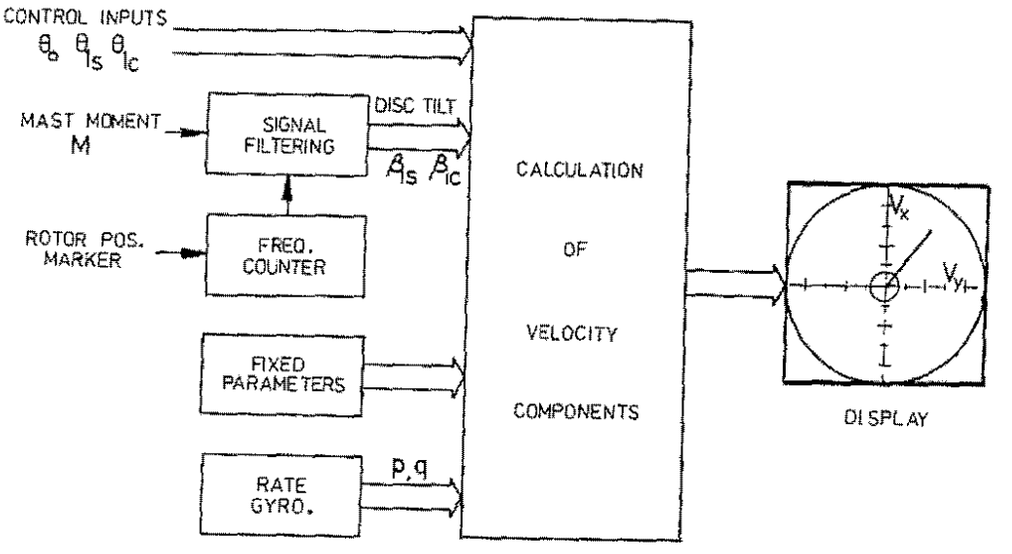

Figure 5 Block Diagramme of System

Figure 6 BO 105 (PAH-1)

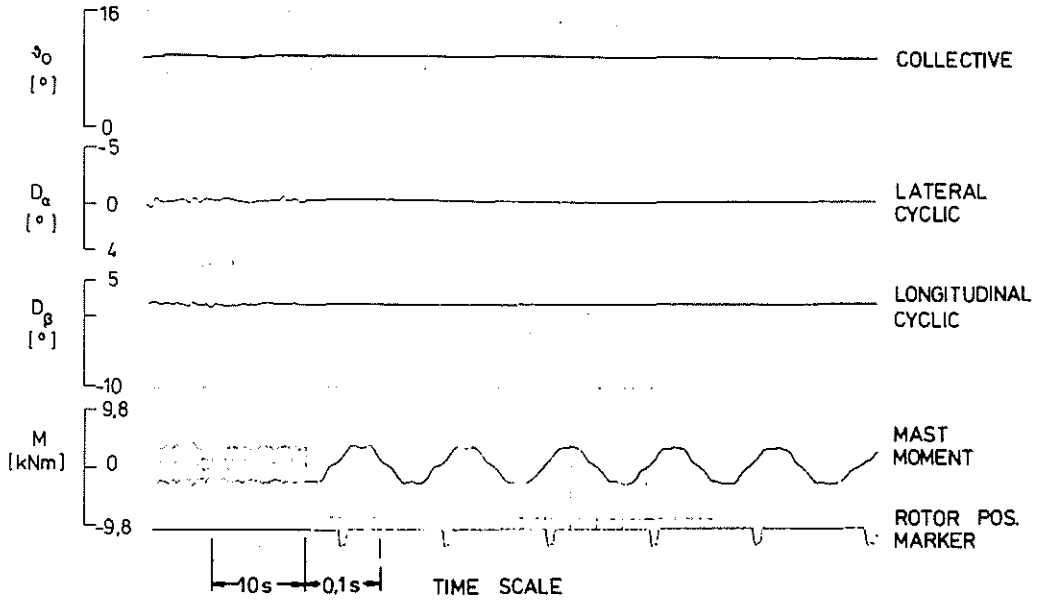

Figure 7 Typical Measurements of Control Positions

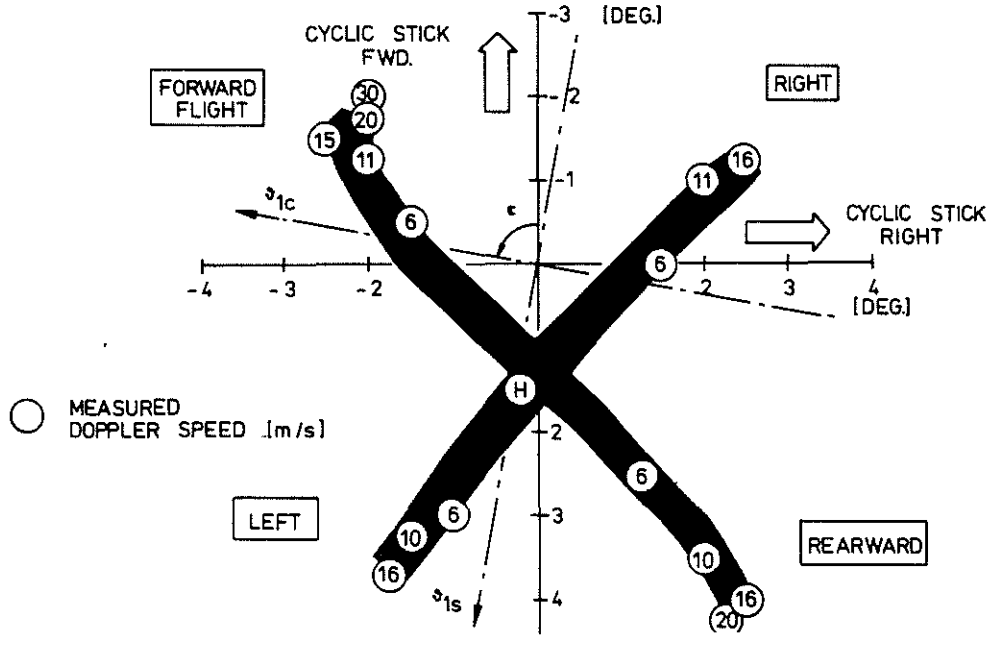

Figure 8 Measured Cyclic Trim Angle (Fwd. Centre of Mass)

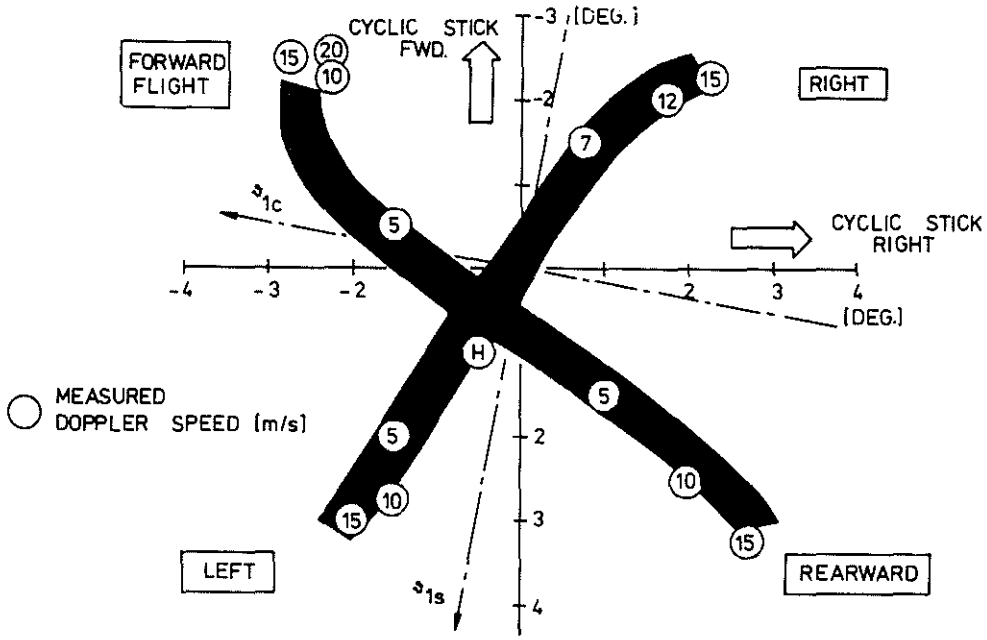

Figure 9 Measured Cyclic Trim Angle (Aft. Centre of Mass)

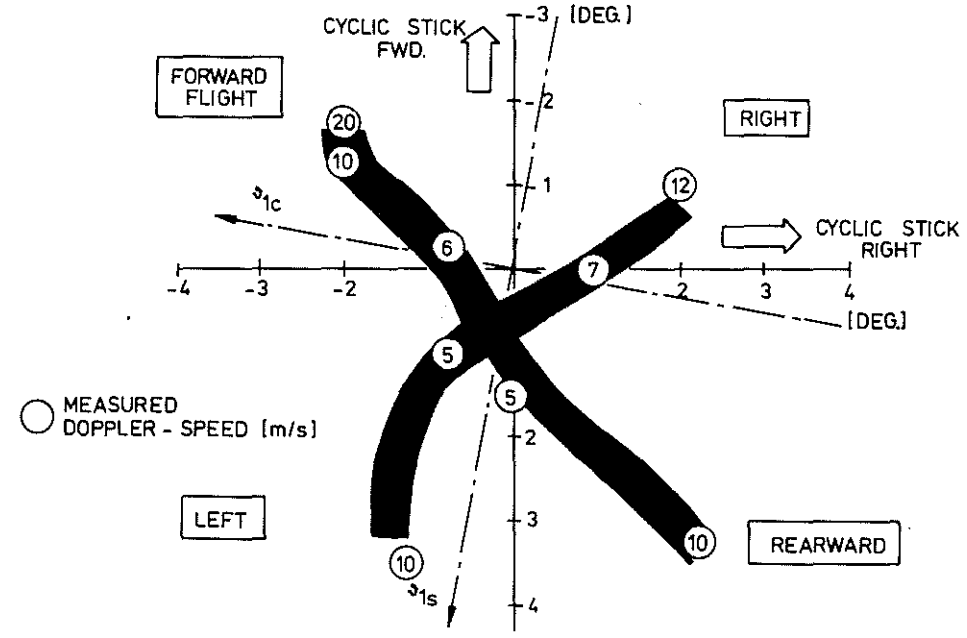

Figure 10 Measured Cyclic Trim Angle in Ground Effect

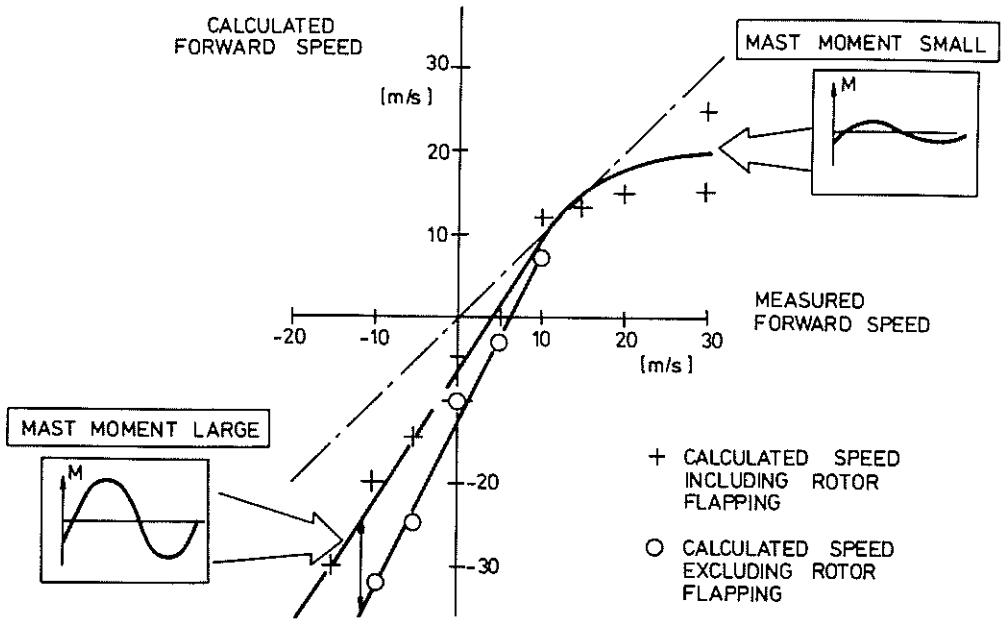

Figure 11 Calculated Forward Speed Against Measured Forward Speed

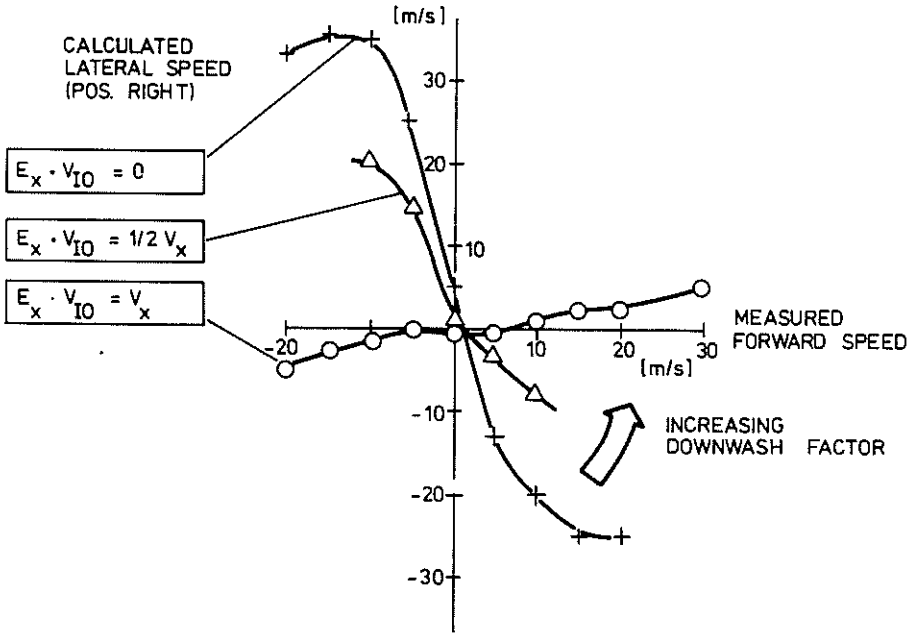

Figure 12 Calculated Lateral Speed Showing Influence of Downwash Factor

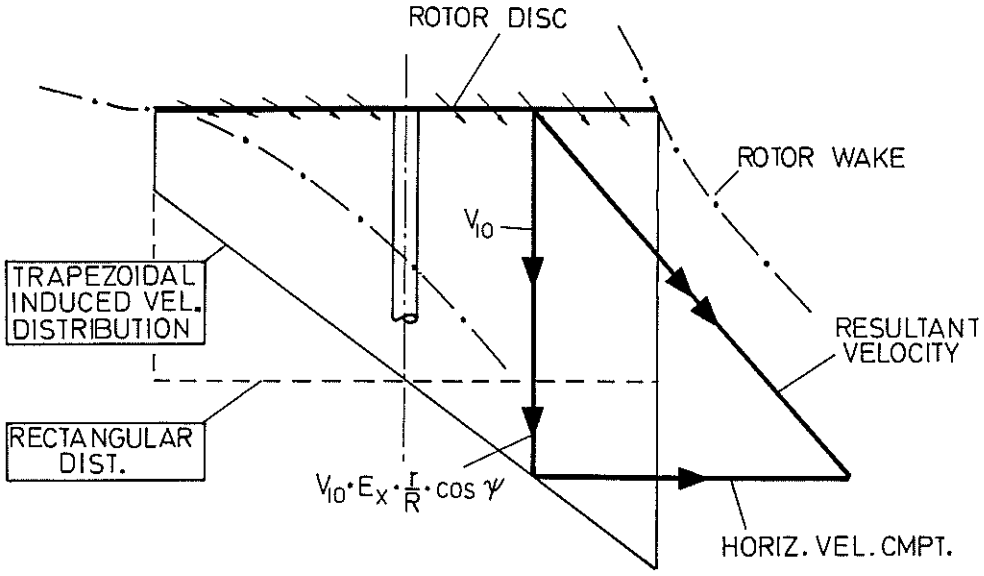

Figure 13 Aerodynamic Flow through the Rotor

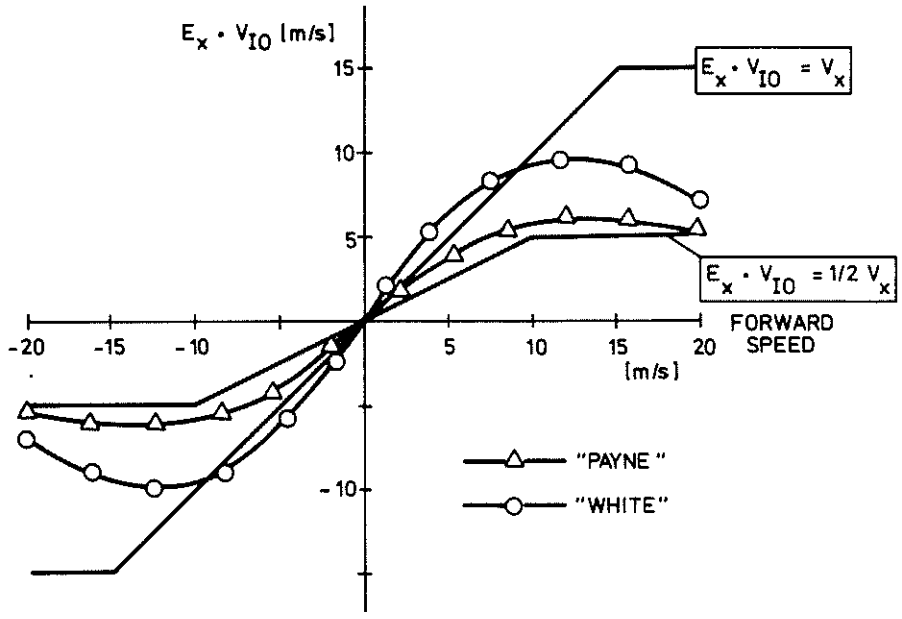

Figure 14 Downwash Factor

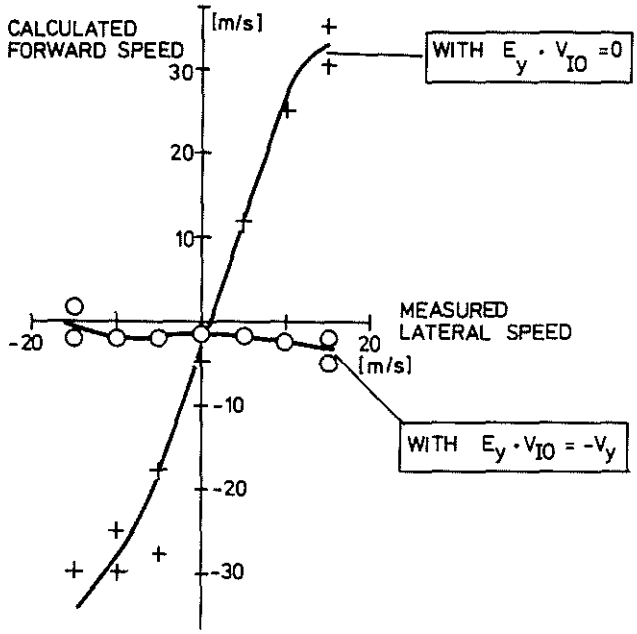

Figure 15 Calculated Forward Speed (Sideways Flight)

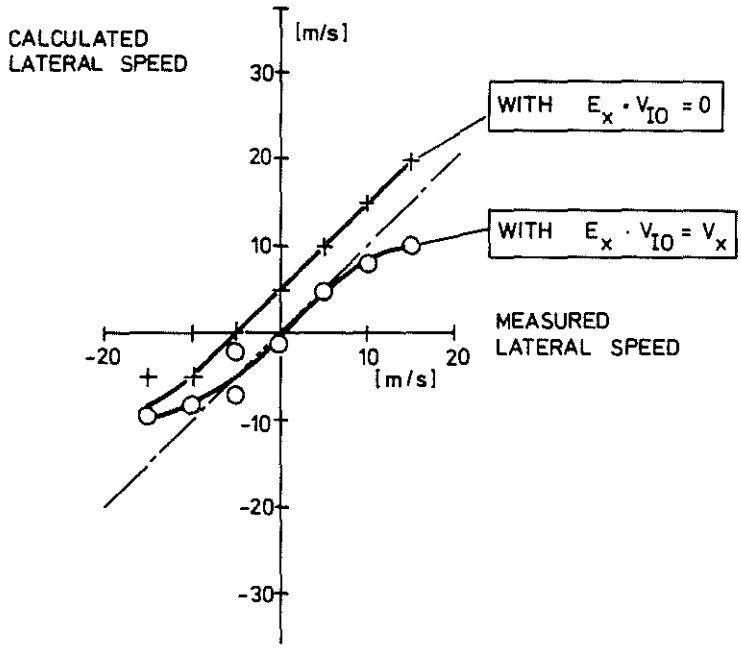

Figure 16 Calculated Lateral Speed (Sideways Flight)

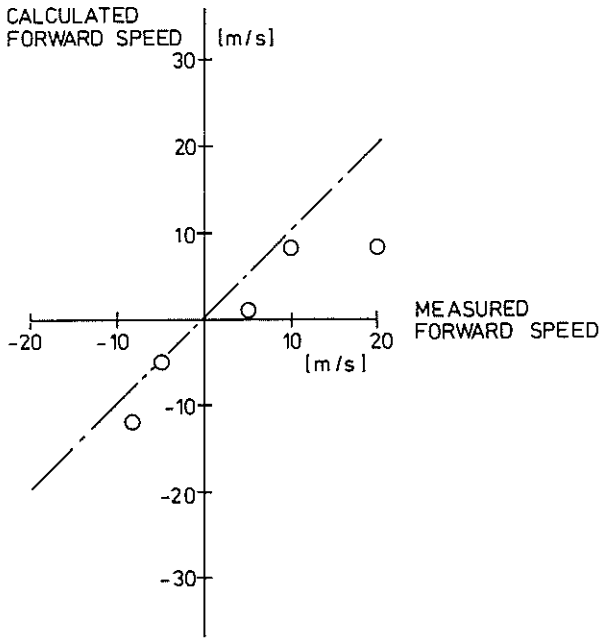

Figure 17 Calculated Forward Speed (In Ground Effect)

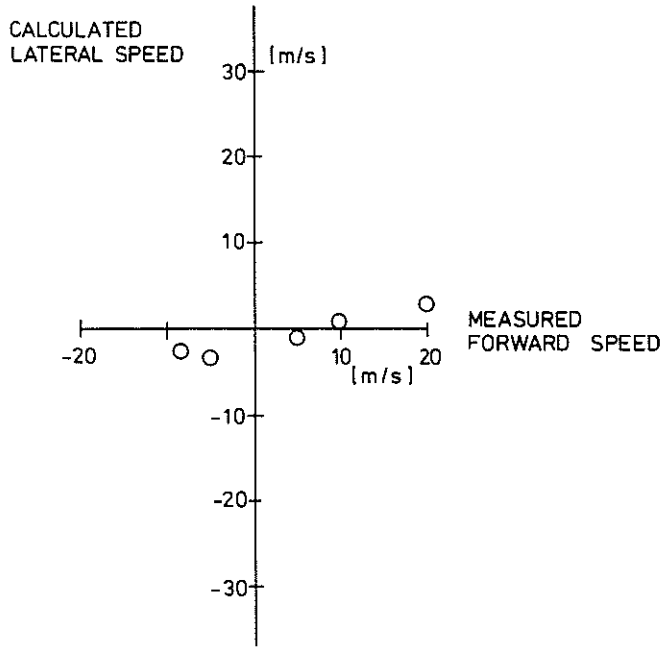

Figure 18 Calculated Lateral Speed (In Ground Effect)

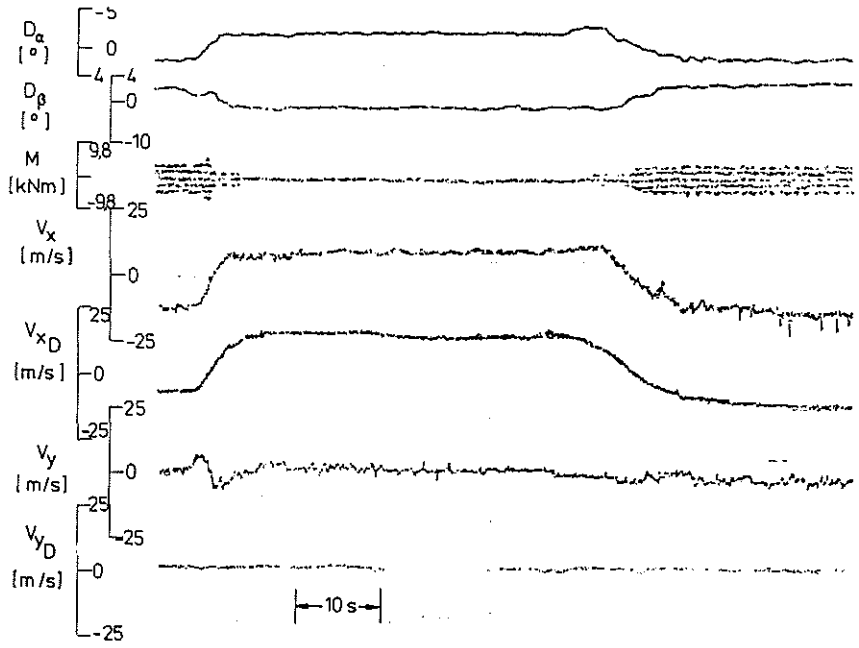

Figure 19 Dynamic Response in Forward Flight

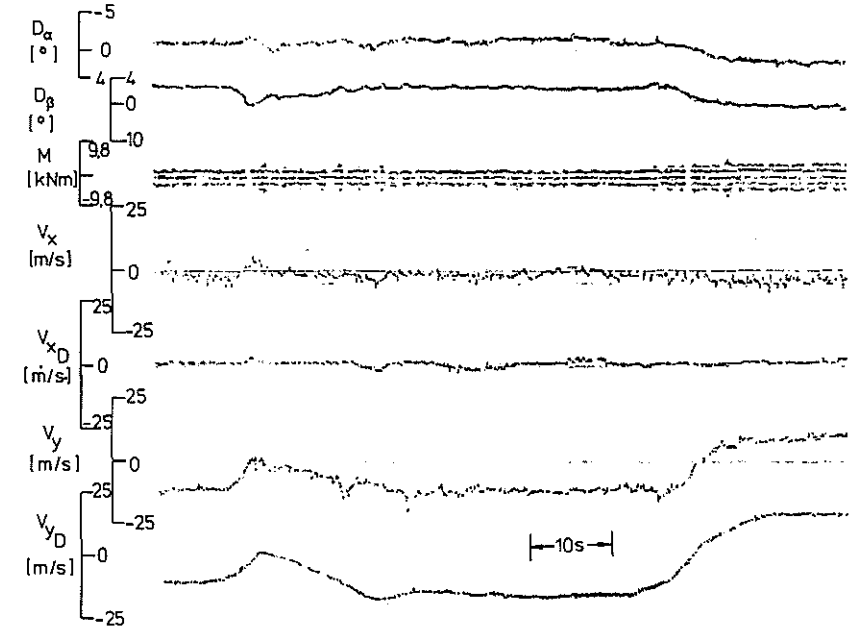

Figure 20 Dynamic Response in Sideways Flight

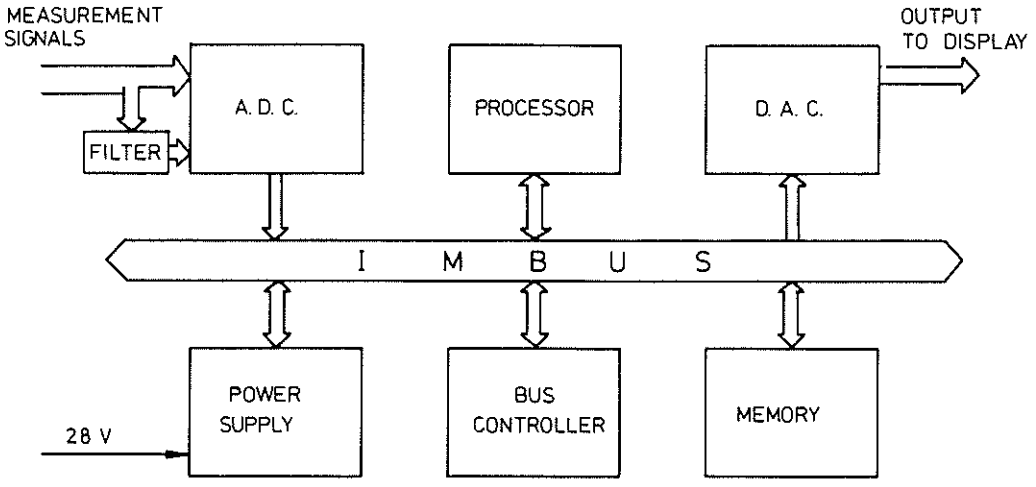

Figure 21 Computer Structure (MODUS)

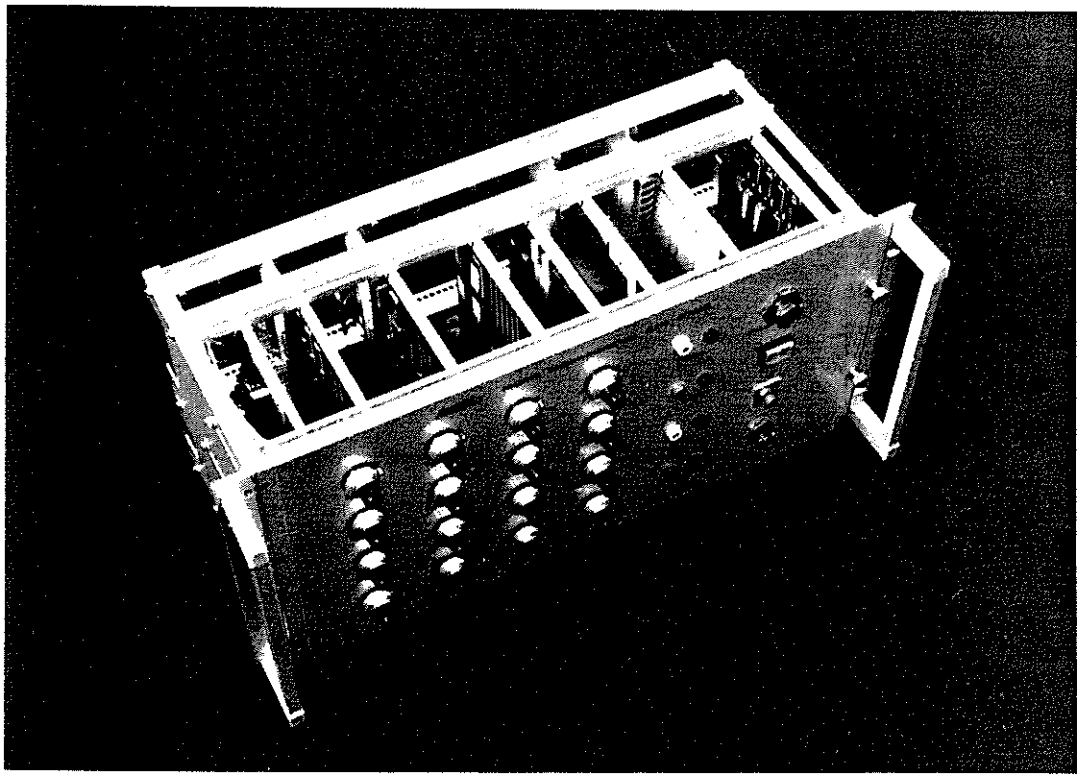

Figure 22 MODUS Computer